

## Chapter 11

### BACKWARD-WAVE OSCILLATORS AND AMPLIFIERS

Let us consider the operation of the traveling-wave tube shown in Figure 11-1. This tube uses a helix as the slow-wave structure with input and output connections to coaxial lines. In contrast to the forward-wave amplifier, this tube has an rf signal impressed onto the helix at the collector end, with

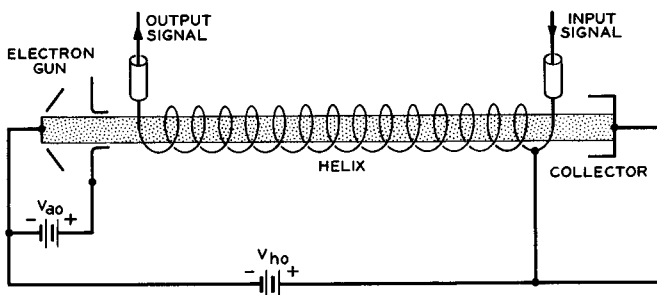


FIG. 11-1 A traveling-wave tube in operation as a backward-wave amplifier. A separate power supply connected to the anode permits beam current control independent of the helix voltage.

the signal output at the gun end. Separate power supplies are provided for the anode and the helix. This provides a means for adjusting the beam current independent of the helix voltage. The beam is assumed to be confined by a strong axial magnetic field.

The helix voltage  $V_{ho}$  is adjusted to a value less than that normally used for forward-wave amplification. Assume  $V_{ho}$  corresponds to an electron velocity  $u_o$  such that a plot of  $ka$  vs.  $\omega L/u_o = \beta_e L$  gives the line  $OA$

in Figure 11-2. At the point of intersection of this line with the  $-1$  space harmonic, the space-harmonic phase velocity is equal to the electron velocity, and some sort of synchronous interaction is to be expected. Since the group velocity for this space harmonic is opposite to the direction of electron travel, we would not expect the interaction to be the same as that described in the preceding chapter.

Let us consider an electron on the outer edge of the electron beam at such a radius that it nearly grazes the helix. Alternatively, we could consider an electron in a thin hollow beam of essentially the helix diameter. We shall assume that the helix is wound from a thin flat tape of metal. The electron sees rf axial electric field due to the helix while passing the gap between adjacent turns of the tape, and zero axial field when passing adjacent to a tape. We may consider these gaps as points of interaction between the beam and the helix.

The helix-beam coupled system effectively comprises a system of feedback loops as indicated in Figure 11-3.  $\theta_1$  is the total phase shift around a loop

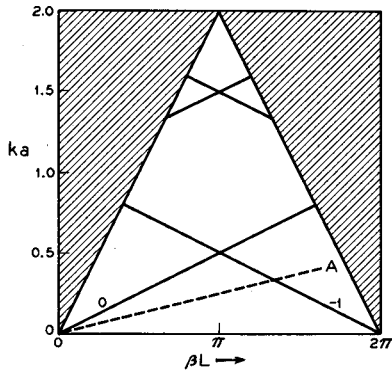


FIG. 11-2 Brillouin diagram for a tape helix. The helix radius and pitch are given by the symbols  $a$  and  $L$ , respectively. The slope of the line  $OA$  is proportional to the square root of the helix voltage.

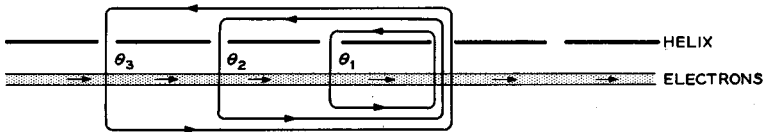


FIG. 11-3 Electrons adjacent to a tape helix interacting with the fields in the helix gaps.  $\theta_1$ ,  $\theta_2$ , and  $\theta_3$  denote loop phase shifts for one, two, and three periods, respectively.

encompassing one period  $L$  of the helix,  $\theta_2$  two periods, etc., for a frequency corresponding to the intersection of line  $OA$  with the  $-1$  space harmonic in Figure 11-2. The circuit is propagating a wave to the left with a fundamental phase shift  $\beta_0 L$  per period at this frequency, due to the impressed signal. Since  $\beta_0 L$  is the phase change in the rf signal which occurs when the beam travels a distance  $L$ , we have

$$\begin{aligned}
 \theta_1 &= \beta_e L + \beta_o L \\
 \theta_2 &= 2(\beta_e L + \beta_o L) \\
 \theta_3 &= 3(\beta_e L + \beta_o L), \text{ etc.}
 \end{aligned}
 \tag{11-1}$$

From Figure 11-2 we observe that  $\beta_{-1}L$  and  $\beta_o L$  are related numerically by

$$\beta_{-1}L = 2\pi - \beta_o L \tag{11-2}$$

Under the condition of synchronism, this must be equal to  $\beta_e L$ ,

$$\beta_e L = 2\pi - \beta_o L \tag{11-3}$$

Introducing this expression into Equations (11-1), we obtain

$$\begin{aligned}
 \theta_1 &= 2\pi \\
 \theta_2 &= 4\pi \\
 \theta_3 &= 6\pi, \text{ etc.}
 \end{aligned}
 \tag{11-4}$$

The total loop phase shift for each of the feedback loops is an integral multiple of  $2\pi$  radians. Hence, the tube will oscillate provided that the gain per feedback loop is sufficient. If the gain is not sufficient for oscillation, the tube acts as a narrow band regenerative amplifier. If the tube is used as an oscillator, there is no need for an impressed signal at the collector end of the helix. Oscillations are generated in the usual manner; that is, an infinitesimal noise signal at the proper frequency builds up because of the positive feedback until a stable operating point is reached.

If the tube of Figure 11-1 is to be used as an oscillator, the rf input signal is replaced by a passive termination, and operation proceeds in the following manner. The beam current is increased from zero by increasing the anode voltage  $V_{ao}$ , with  $V_{ho}$  held constant. As the beam current increases, the gain per feedback loop also increases. Finally, a point is reached where the tube breaks into oscillation. The dc beam current corresponding to this point is termed the starting current,  $I_{ST}$ .

Since there are many feedback loops, it is not necessary that each one have a loop gain equal to unity for oscillations to be produced. In fact, we should expect the starting current to vary inversely with the number of feedback loops or the length of the helix. We shall find that oscillations are produced when the product of the gain per wavelength along the helix times the number of circuit wavelengths exceeds some critical value. In terms of the traveling-wave tube parameters introduced in the preceding chapter, this product is proportional to  $CN$ .

A traveling-wave tube operated in this manner is known as a backward-wave oscillator. The rf output power is taken from the electron gun end of the helix. In external physical appearance it is very similar to a traveling-wave amplifier; the helix is usually shorter and larger in diameter, and there is no circuit sever or loss pattern.

The frequency of oscillation is tuned electronically by varying the helix voltage. This is easily seen by referring to Figure 11-2. Changing the beam voltage changes the frequency corresponding to the intersection of the line  $OA$  with the  $-1$  space harmonic. Extremely wide electronic tuning ranges are obtainable; typically, the ratio of the highest to the lowest frequency is two to one.

With the beam current adjusted to a value below the starting current, the tube is usable as a backward-wave amplifier. RF power introduced at the collector end of the helix is amplified and delivered out the gun end. Because of the regenerative nature of the amplification process, extremely narrow fractional bandwidths are obtained, of the order of 0.5 per cent. The frequency of amplification is tuned electronically by varying the helix voltage. In systems requiring a highly selective, electronically tunable amplifier the backward-wave amplifier is unexcelled.

In the following sections we shall examine the quantitative aspects of these devices. Both oscillation and amplification modes of behavior are derived from the same basic theory, which is closely related to the theory of the preceding chapter.

### 11.1 Theory of Backward-Wave Interaction

The theory of backward-wave interaction closely parallels that given for the traveling-wave amplifier in Section 10.1. An electronic equation and a circuit equation are derived individually and then solved simultaneously to determine allowed values for the "hot" propagation constants.

#### (a) *The Electronic Equation*

This equation expresses the electron motion induced by a space harmonic of the circuit field traveling synchronously with the electrons. It is given by Equation (10.1-18) for backward waves as well as for forward waves. It should be clear that synchronism refers to the equality of the electron velocity and the space-harmonic *phase velocity*; no condition is placed on the space-harmonic *group velocity*.

#### (b) *The Circuit Equation*

This equation expresses the manner in which currents are induced into the slow-wave structure by the beam convection currents and the way in which these induced currents propagate and combine.

This equation is derived with reference to Figure 10.1-1. In the case of backward-wave interaction, the arrows above the circuit refer to the direction of the *group velocity*, the direction of energy propagation, for each

of the waves shown. In the traveling-wave amplifier there was no ambiguity since the phase and group velocities were in the same direction. The convection current segment in the beam induces power into the circuit, giving rise to incremental waves having group velocities directed away from the point of induction.

With this interpretation in mind, the development of Section 10.1(b) follows exactly for backward-wave interaction up to and including Equation (10.1-27). We shall proceed with the development from this point.

Let  $\Gamma_o = -\alpha + j\beta_n$  be the complex cold circuit propagation constant for a synchronous backward-wave space harmonic with positive phase velocity and negative group velocity. The  $-1$  space harmonic shown in Figure 11-2 is of this type. Such a wave has a  $z$  dependence of the form

$$\epsilon^{-\Gamma_o z} = \epsilon^{\alpha z} \epsilon^{-j\beta_n z} \quad (11.1-1)$$

with  $\alpha$  and  $\beta_n$  both positive. We note that the wave amplitude is attenuated in the minus  $z$  direction corresponding to the direction of power flow.

In order to include the possibility of a backward-wave amplifier we assume that energy is introduced onto the circuit from an external signal source at the collector end. The total space-harmonic field at an arbitrary point ( $z = a$ ) on the circuit is then given by the superposition of three contributions as follows:

A. The power coming from the external source at the collector end of the circuit ( $z = l$ ),

$$E_{znA}(a) = E_{zn0} \epsilon^{\Gamma_o(l-a)} \quad (11.1-2)$$

where  $E_{zn0}$  is the value of the space harmonic at  $z = l$  corresponding to this power.

B. The superposition of the incremental waves  $dE_{zn+}$  arriving at  $z = a$  from the left are given by

$$E_{znB}(a) = \int_0^a \epsilon^{\Gamma_o(a-z)} dE_{zn+} \quad (11.1-3)$$

C. The superposition of the incremental waves  $dE_{zn-}$  arriving at  $z = a$  from the right are given by

$$E_{znC}(a) = \int_a^l \epsilon^{\Gamma_o(z-a)} dE_{zn-} \quad (11.1-4)$$

In all cases we note that the waves advance in phase and decay in amplitude from the point of origin, characteristic of backward waves.

The total field at  $z = a$  is obtained by summing the above three contribu-

tions and making use of Equation (10.1-27):

$$E_{zn}(a) = E_{zn0}\epsilon^{\Gamma_0(l-a)} - \frac{1}{2}\beta_n^2 K_n \int_0^a i\epsilon^{\Gamma_0(a-z)} dz - \frac{1}{2}\beta_n^2 K_n \int_a^l i\epsilon^{\Gamma_0(z-a)} dz \tag{11.1-5}$$

where  $i$  is the ac convection current in the electron beam. The variable of integration is replaced by  $\tau$ , and  $a$  is replaced by  $z$ , a variable point, obtaining

$$E_{zn}(z) = E_{zn0}\epsilon^{-\Gamma_0(z-l)} - \frac{1}{2}\beta_n^2 K_n \int_0^z i(\tau)\epsilon^{\Gamma_0(z-\tau)} d\tau - \frac{1}{2}\beta_n^2 K_n \int_z^l i(\tau)\epsilon^{-\Gamma_0(z-\tau)} d\tau \tag{11.1-6}$$

This equation can be differentiated twice to obtain

$$\Gamma^2 E_{zn} = \Gamma_0^2 E_{zn0}\epsilon^{-\Gamma_0(z-l)} - \frac{1}{2}\Gamma_0^2 \beta_n^2 K_n \int_0^z i(\tau)\epsilon^{\Gamma_0(z-\tau)} d\tau - \frac{1}{2}\Gamma_0^2 \beta_n^2 K_n \int_z^l i(\tau)\epsilon^{-\Gamma_0(z-\tau)} d\tau - \Gamma_0 \beta_n^2 K_n i \tag{11.1-7}$$

where it has been assumed that the resultant space harmonic has a “hot”  $z$  dependence of the form

$$\epsilon^{-\Gamma z}$$

The last two equations are combined to yield the *circuit equation* for backward-wave interaction:

$$(\Gamma^2 - \Gamma_0^2)E_{zn} = -\Gamma_0 \beta_n^2 K_n i \tag{11.1-8}$$

This differs from the corresponding forward-wave amplifier equation, Equation (10.1-34), only in the sign of the term containing the impedance.

(c) *Solutions for Cumulative Interaction*

Allowed values of the “hot” propagation constant  $\Gamma$  are determined from a simultaneous solution of the electronic and circuit equations. One obtains

$$(\Gamma^2 - \Gamma_0^2) \left[ (\Gamma - j\beta_0)^2 + \frac{\omega_d^2}{u_0^2} \right] = -\frac{j\beta_d \beta_n^2 \Gamma_0 K_n I_0}{2V_0} \tag{11.1-9}$$

This equation is simplified by introducing certain parameters.  $C$  and  $QC$  are defined as in Equations (10.1-36) and (10.1-37).  $b$  and  $d$  are defined by

$$\Gamma_0 \equiv j\beta_0(1 + Cb + jCd) \tag{11.1-10}$$

and  $\delta$  is defined by Equation (10.1-39). Equations (10.1-40) and (10.1-41)

are correct as written for backward-wave interaction. Equation (11.1-9) simplifies to

$$\delta^2 = \frac{1}{b + jd - j\delta} - 4QC \quad (11.1-11)$$

Equation (11.1-11) determines three allowed values for the "hot" propagation constant in terms of the various operating parameters of the tube. The various fields and beam quantities may thus be written as a superposition of three waves, as in Equations (10.1-53). The boundary conditions at  $z = 0$  for these various quantities are the same as in the forward-wave amplifier, as indicated in Equations (10.1-60). It should be noted that  $E_{zn}(0)$  corresponds to the rf output power for backward-wave interaction, and we have not so far determined its value explicitly. Nonetheless, we can solve Equation (10.1-60) to determine the values of  $E_{zT1}$ ,  $E_{zT2}$ , and  $E_{zT3}$  in terms of  $E_{zn}(0)$ . Thus, we obtain Equation (10.1-61) and similar expressions for  $E_{zT2}$  and  $E_{zT3}$  by permuting the subscripts.

It will be most convenient to write all of our equations in terms of the waves corresponding to the space-harmonic field due to the circuit. Combining Equations (10.1-61) and (10.1-73), we obtain

$$\frac{E_{zn1}}{E_{zn}(0)} = \frac{\delta_1^2 + 4QC}{(\delta_1 - \delta_2)(\delta_1 - \delta_3)} \quad (11.1-12)$$

with expressions for  $E_{zn2}$  and  $E_{zn3}$  obtained by permuting subscripts. The total space-harmonic field at any axial position is given by

$$E_{zn}(z) = E_{zn1}\epsilon^{-\Gamma_1 z} + E_{zn2}\epsilon^{-\Gamma_2 z} + E_{zn3}\epsilon^{-\Gamma_3 z} \quad (11.1-13)$$

Using Equation (11.1-12) and similar expressions for  $E_{zn2}$  and  $E_{zn3}$ , we obtain at  $z = l$ :

$$\begin{aligned} \frac{E_{zn}(l)}{E_{zn}(0)} &= \frac{\delta_1^2 + 4QC}{(\delta_1 - \delta_2)(\delta_1 - \delta_3)}\epsilon^{-\Gamma_1 l} + \frac{\delta_2^2 + 4QC}{(\delta_2 - \delta_3)(\delta_2 - \delta_1)}\epsilon^{-\Gamma_2 l} \\ &\quad + \frac{\delta_3^2 + 4QC}{(\delta_3 - \delta_1)(\delta_3 - \delta_2)}\epsilon^{-\Gamma_3 l} \end{aligned} \quad (11.1-14)$$

The definitions given by Equations (10.1-39) and (10.1-70) are substituted into this equation, obtaining

$$\begin{aligned} \frac{E_{zn}(l)}{E_{zn}(0)}\epsilon^{j2\pi N} &= \frac{\delta_1^2 + 4QC}{(\delta_1 - \delta_2)(\delta_1 - \delta_3)}\epsilon^{2\pi\delta_1 CN} + \frac{\delta_2^2 + 4QC}{(\delta_2 - \delta_3)(\delta_2 - \delta_1)}\epsilon^{2\pi\delta_2 CN} \\ &\quad + \frac{\delta_3^2 + 4QC}{(\delta_3 - \delta_1)(\delta_3 - \delta_2)}\epsilon^{2\pi\delta_3 CN} \end{aligned} \quad (11.1-15)$$

The gain of a backward-wave amplifier is given by

$$\text{gain} = 20 \log \left| \frac{E_{zn}(0)}{E_{zn}(l)} \right| \text{ db} \quad (11.1-16)$$

which may be calculated directly from Equation (11.1-15). The gain is seen to be a function of  $QC$  and  $CN$  directly and of  $b$ ,  $d$ , and  $QC$  indirectly, since the latter quantities determine the values of the  $\delta$ 's. We shall further consider the backward-wave amplifier in a later section.

As the value of the right-hand side of Equation (11.1-15) approaches zero, the backward-wave amplifier gain approaches infinity. At this point the tube will oscillate, since a finite value of  $E_{zn}(0)$  is obtainable for a vanishingly small value of  $E_{zn}(l)$ . Thus, the threshold conditions for oscillation are given by the solution of the equation

$$\frac{\delta_1^2 + 4QC}{(\delta_1 - \delta_2)(\delta_1 - \delta_3)} \epsilon^{2\pi\delta_1 CN} + \frac{\delta_2^2 + 4QC}{(\delta_2 - \delta_3)(\delta_2 - \delta_1)} \epsilon^{2\pi\delta_2 CN} + \frac{\delta_3^2 + 4QC}{(\delta_3 - \delta_1)(\delta_3 - \delta_2)} \epsilon^{2\pi\delta_3 CN} = 0 \quad (11.1-17)$$

Since this equation has real and imaginary parts, there are in reality two simultaneous equations to be solved. Thus, two conditions are determined. One condition is  $CN$ , a quantity which we may interpret loosely as the product of gain per wavelength times the number of circuit wavelengths. This interpretation is based upon assuming an analogy to forward-wave amplifier theory, whereas in reality Equation (11.1-15) shows that backward-wave amplifier gain is given by an extremely complicated expression, not simply proportional to  $CN$ . The other condition determined by Equation (11.1-17) is  $b$ , the degree of synchronism between the beam and the space harmonic. This condition is analogous to the phase condition in oscillator theory. For a given helix voltage, this condition determines the frequency of oscillation precisely.

Solutions for the backward-wave oscillator starting conditions are not easily obtained. This is due to the fact that the values of the  $\delta$ 's are by Equation (11.1-11) functions of  $b$  and  $C$ , which are unknowns. Thus, Equations (11.1-11) and (11.1-17) must be solved simultaneously, a task accomplished most readily with an analogue computer.

Let us examine the nature of the solutions in two simple cases. First, we assume zero space charge ( $QC = 0$ ) and zero circuit loss ( $d = 0$ ). The start-oscillation conditions are from computer calculations:<sup>1</sup>

$$\begin{aligned} CN &= 0.314 \\ b &= 1.522 \end{aligned} \quad (11.1-18)$$

For a given helix voltage on a particular tube, the first condition in effect determines the beam current above which oscillations are produced. The second condition determines the exact frequency of oscillation. The cor-

---

<sup>1</sup>Reference 11.1.



responding values of  $\delta$  are

$$\begin{aligned}\delta_1 &= 0.725 + j0.150 \\ \delta_2 &= -0.725 + j0.150 \\ \delta_3 &= 0.083 - j1.796\end{aligned}\quad (11.1-19)$$

Phasors representing the three waves are shown in Figure 11.1-1. These phasors are derived from Equation (11.1-12) and the appropriate values of  $\delta$ .

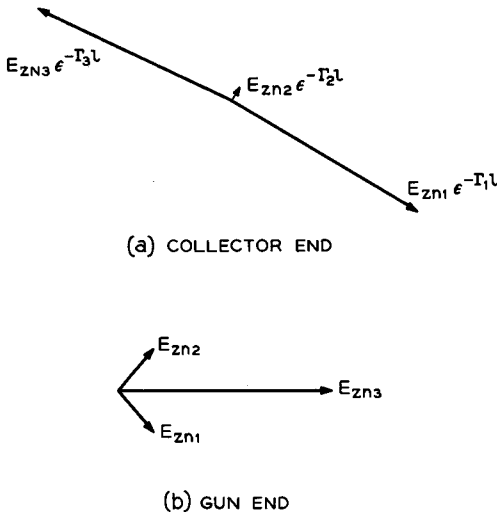


FIG. 11.1-1 Phasor diagrams for the three waves in a backward-wave oscillator with  $QC = d = 0$ . (a) Waves at the collector end of the helix; these waves add to zero. (b) Waves at the gun end of the helix; these waves add to produce the output signal.

At the collector end of the circuit, the three phasors add to zero. As these waves propagate from the collector end to the gun end, they experience differential phase shift and different degrees of amplitude change by Equations (11.1-19) so as to obtain a non-zero resultant field at the gun end. The only wave that grows in this direction is  $E_{zn2}$ , and we see from Figure 11.1-1 that this contributes only slightly to the total field at the gun end. Thus, backward-wave interaction is seen to be principally an interference effect between various waves rather than a growing-wave phenomenon as in the forward-wave amplifier. The conditions in a backward-wave amplifier are similar to those shown in Figure 11.1-1; in this case, the three waves at the collector end do not quite add to zero.

As a second example, we consider the solutions for large space charge ( $QC > 0.25$ ) and zero circuit loss ( $d = 0$ ). Under these conditions it can be shown<sup>2</sup> that the start-oscillation conditions are

$$\begin{aligned}
 CN &\cong \frac{1}{2}(QC)^{1/4} \\
 b &\cong \sqrt{4QC}
 \end{aligned}
 \tag{11.1-20}$$

and the corresponding values of  $\delta$  are

$$\begin{aligned}
 \delta_1 &\cong -j\sqrt{4QC}[1 - \frac{1}{4}(QC)^{-3/4}] \\
 \delta_2 &\cong j\sqrt{4QC} \\
 \delta_3 &\cong -j\sqrt{4QC}[1 + \frac{1}{4}(QC)^{-3/4}]
 \end{aligned}
 \tag{11.1-21}$$

$\delta_2$  corresponds to the fast space-charge wave, as in Equation (10.1-51). This wave is negligible in amplitude compared with the other two waves. The phasor diagrams for the three waves are shown in Figure 11.1-2 for  $QC = 1$ . We see that for large space charge we may think of the backward-wave oscillator circuit field as given by the interference of two waves. At the collector end they are 180 degrees out of phase, whereas differential phase shift causes them to be in phase at the gun end.

Accurate computations have been made of the start-oscillation conditions over the useful ranges of space charge and circuit loss.<sup>3</sup> These results are presented in Figures 11.1-3 and 11.1-4. These curves are used as follows. For a given helix voltage the ratio  $Q/N$  is calculated (both  $Q$  and  $N$  are independent of beam current)<sup>4</sup>.  $CN$  for start oscillations is obtained from Figure 11.1-3. Then  $b$  is calculated from Figure 11.1-4 and the known value of  $CN$ . The beam current can be calculated from the value of  $CN$  and the known values of beam-coupling impedance, beam diameter, etc. This procedure gives the start-

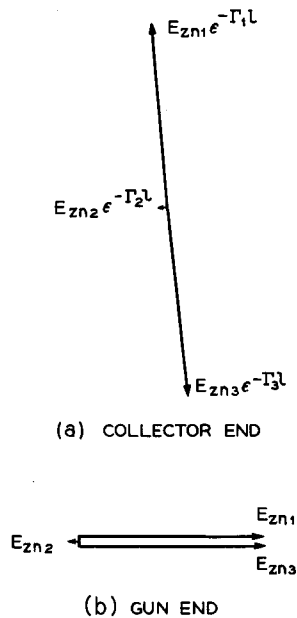


FIG. 11.1-2 Phasor diagrams for the three waves at the two ends of the helix of a backward-wave oscillator with  $QC = 1, d = 0$ . (a) Collector end. (b) Gun end.

<sup>2</sup>Reference 11.1. Equations (11.1-21) were not correct as originally published.

<sup>3</sup>*Ibid.*

<sup>4</sup>See Problem 10.2.

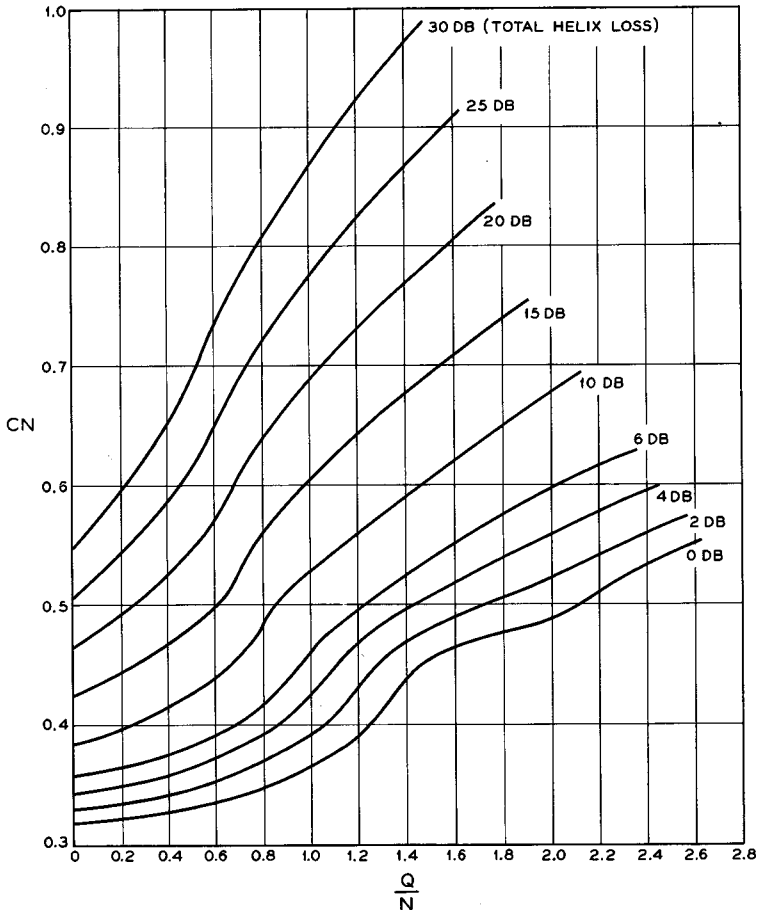


FIG. 11.1-3 Oscillations are produced in a backward-wave oscillator for values of  $CN$  equal to or greater than the value given above. Its value is a function of the space-charge parameter and the total circuit loss (Reference 11.1). (Courtesy of *Proceedings IRE*)

ing current at one frequency; it is repeated to determine the starting conditions at other frequencies.

The above theory and results apply only at the threshold of oscillation. The equations were derived on the basis that all rf beam perturbations are extremely small so that the various physical equations are all linear.<sup>5</sup> As

<sup>5</sup>This was discussed in connection with Equations (9.3-12) and (10.1-12).

the beam current is increased above the starting current, the level of oscillation is limited by nonlinear effects in the beam kinematics. The output power increases with beam current and the oscillation frequency decreases slightly; the latter effect is known as frequency pushing.

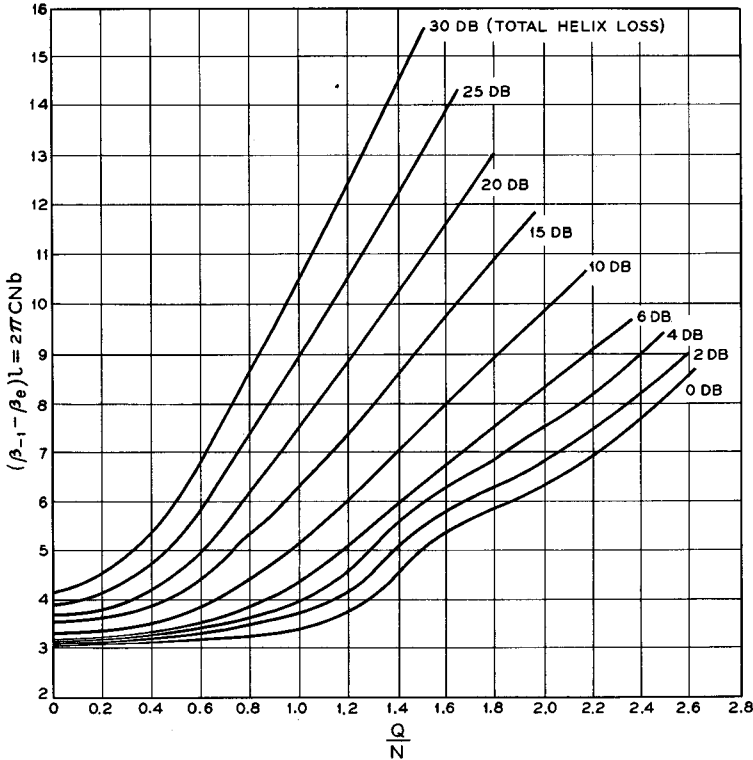


FIG. 11.1-4 Curves determining  $b$  in a backward-wave oscillator at start oscillation as a function of the space-charge parameter and circuit attenuation.  $b$  determines the exact frequency of oscillation, using Equation (10.1-40) (Reference 11.1). (Courtesy of *Proceedings IRE*)

Another effect that may appear at higher beam currents is a higher mode of oscillation. This mode is predicted as the next higher-order solution of the transcendental Equation (11.1-17). Since this mode requires a beam current related to the main-mode starting current by a factor of eight or greater, it is not obtained under normal operating conditions.

The rf power output cannot be predicted from the linear theory presented here. A combined theoretical-empirical analysis has been made to

determine this important quantity.<sup>6</sup> The results are that the maximum electronic efficiency is given by

$$\eta_e \cong 1.3C \quad (11.1-22)$$

for small space charge ( $QC < 0.5$ ) and by

$$\eta_e \cong \frac{\omega_q}{\omega}$$

for large space charge ( $QC > 0.5$ ), where  $C$  and  $\omega_q$  are calculated at the operating value of beam current, which is somewhat larger than the starting current. Since  $C$  and  $\omega_q/\omega$  are typically quite small in these tubes, maximum electronic efficiencies are usually no more than a few per cent. These efficiencies are maximum in the sense that various imperfections in the tube (such as circuit loss and poor circuit match) cause further reduction of the output power.

## 11.2 Backward-Wave Oscillators

The most commonly used slow-wave structure for backward-wave oscillators is the helix. Interaction is with the  $-1$  space harmonic as shown in Figure 11-2.

The characteristics of the Brillouin diagram for the helix have been determined in the preceding chapter. The frequency of oscillation is approximately given by the intersection of the voltage line  $OA$  in Figure 11-2 with the  $-1$  space harmonic. An accurate determination of the frequency requires the use of Equation (10.1-40) together with a knowledge of  $b$  and  $C$ .

Over what frequency range will a typical tube operate? As the helix voltage is increased, the voltage line approaches coincidence with the fundamental space harmonic. This situation occurs at a frequency corresponding to  $ka = 0.5$ . The electrons are in synchronism with two space harmonics simultaneously. If the ends of the helix are not perfectly terminated, reflections are set up which are amplified in both directions, causing erratic behavior in the power output as a function of frequency. This situation is usually avoided by restricting operation to frequencies below this point.

At extremely low frequencies the coupling impedance  $K_{-1}$  drops off rather seriously, as we shall see later. Since there is an upper limit to the beam current,  $CN$  falls below the start-oscillation value, and the tube will not oscillate. Thus, operation is usually restricted to the frequency range from  $ka$  equal to 0.1 or 0.2 up to  $ka$  slightly below 0.5.

<sup>6</sup>Reference 11.2.

Next we shall consider an evaluation of the coupling impedance  $K_{-1}$ . No exact theoretical analysis has been made of this parameter. However, several rather complicated approximate analyses have been made.<sup>7</sup> Follow-

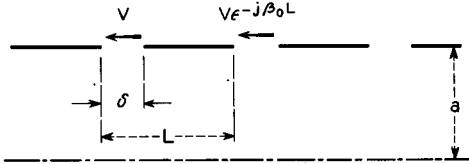


FIG. 11.2-1 Cross section of a thin tape helix obtained by the intersection with the semi-infinite plane given by  $\theta = 0$ .

ing the pattern set up in the previous chapter, we shall present an extremely simple approximate evaluation of  $K_{-1}$  which compares favorably with the more complicated analyses over the useful frequency range of the helix.

Let us consider a thin tape helix. Figure 11.2-1 shows a cross-sectional view of the helix obtained by means of the intersection with the semi-infinite plane  $\theta = 0$ . By Floquet's Theorem the voltages across two successive gaps in this plane differ by the factor  $e^{-j\beta_0 L}$ , assuming negligible circuit attenuation. We consider, for the purpose of this analysis, the set of space harmonics with positive group velocity. Identical results are obtained for the set with negative group velocity.

From Equation (10.3-7) the axial electric field at  $r = a$  and  $\theta = 0$  is given by

$$E_z = \sum_n B_n I_n(\gamma_n a) e^{-j\beta_n z} \tag{11.2-1}$$

We assume that the electric field does not vary with position within the gap. The evaluation of the coefficients  $B_n$  proceeds as in Equations (10.2-15) to (10.2-17), obtaining

$$B_n L I_n(\gamma_n a) = M_{1(n)} V \tag{11.2-2}$$

where  $M_{1(n)}$  is defined by Equation (10.2-20) and  $V$  is the voltage across the gap at  $z = 0$ . Thus, the total axial field within the helix is given by

$$E_z = \frac{V}{L} \sum_n M_{1(n)} \frac{I_n(\gamma_n r)}{I_n(\gamma_n a)} e^{\pm jn\theta} e^{-j\beta_n z} \tag{11.2-3}$$

a summation of space harmonics.

<sup>7</sup>References 11.3, 11.4.

The impedance is evaluated from Equation (10.1-19) as

$$K_{-1} = \frac{\int |E_{z(-1)}|^2 dS}{2\beta_{-1}^2 P S} = \frac{M_{1(-1)}^2 M_{2(-1)}^2 |V|^2}{2\beta_{-1}^2 L^2 P} \quad (11.2-4)$$

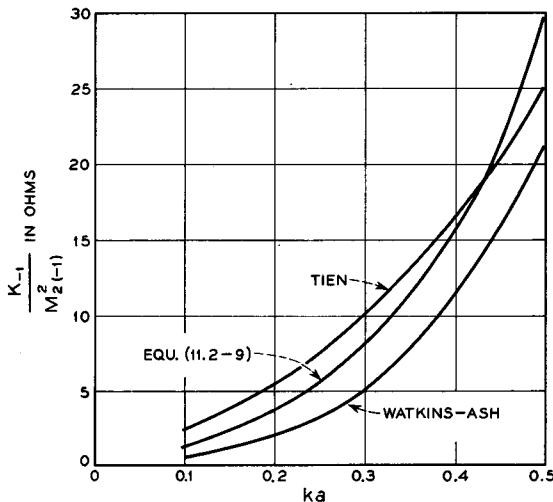


FIG. 11.2-2 Backward-wave impedance of a tape helix for  $\delta/L = 1/3$ . The simplified theory of this chapter is compared with the more complicated theoretical values derived by Tien (Reference 11.4) and Watkins-Ash (Reference 11.3).

where the space-harmonic amplitude is obtained from Equation (11.2-3).  $M_{2(n)}^2$  is defined by the equation

$$M_{2(n)}^2 = \frac{1}{S} \int \frac{I_n^2(\gamma_n r)}{I_n^2(\gamma_n a)} dS \quad (11.2-5)$$

where  $S$  is the beam cross-sectional area, and the integral is taken over the beam cross section.

The impedance for the fundamental is given in the same manner as

$$K_o = \frac{\int |E_{zo}|^2 dS}{2\beta_o^2 P S} = \frac{M_{1(0)}^2 M_{2(0)}^2 |V|^2}{2\beta_o^2 P S} \quad (11.2-6)$$

Combining Equations (11.2-4) and (11.2-6), we obtain

$$K_{-1} = K_o \frac{M_{1(-1)}^2 M_{2(-1)}^2 (\beta_o L)^2}{M_{1(0)}^2 M_{2(0)}^2 (\beta_{-1} L)^2} \quad (11.2-7)$$

relating the beam-coupling impedances of the fundamental and  $-1$  space harmonics. Since we have derived an expression for  $K_o$  in the preceding chapter, this equation enables us to determine  $K_{-1}$ .

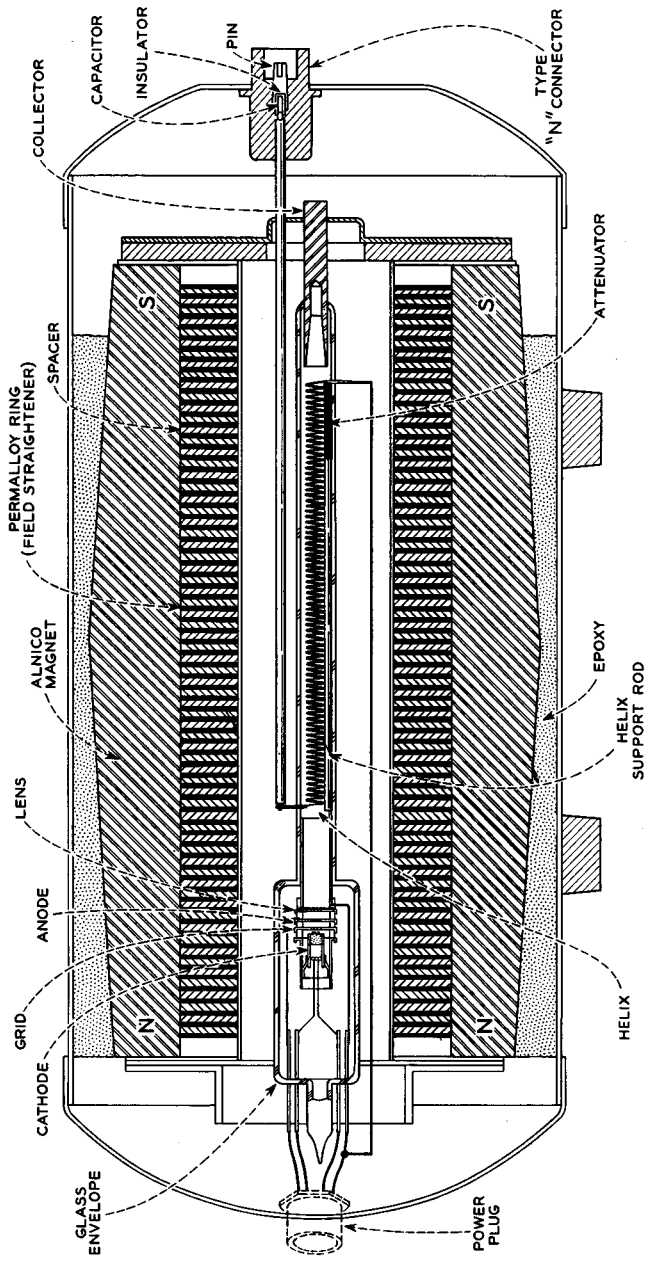


Fig. 11.2-3 SE 201 backward-wave oscillator. Since this tube is operated with the cathode at ground potential, an insulator is provided in the rf output connector to isolate the high voltage on the helix. (Courtesy of Stewart Engineering Co.)



From Figure 11-2 we have the following relationships:

$$\begin{aligned} \beta_o L &= 2\pi ka \\ \beta_{-1} L &= 2\pi(1 - ka) \end{aligned} \tag{11.2-8}$$

These relations are inserted into Equation (11.2-7) together with Equation (10.3-22) for  $K_o$  to obtain

$$K_{-1} = M_{2(-1)}^2 \frac{15(ka)^3}{(1 - ka)^4} \frac{\sin^2 \frac{\pi\delta}{L}(1 - ka)}{\sin^2 \frac{\pi\delta}{L}ka} \text{ohms} \tag{11.2-9}$$

This is plotted in Figure 11.2-2 as a function of  $ka$  for  $\delta/L = \frac{1}{3}$ . Also plotted are the results of two other analyses.<sup>8</sup> A comparison of these three results tends to substantiate the approximate analysis we have used.

The radial variation of the  $-1$  space-harmonic field is proportional to the function  $I_1(\gamma_1 r)$ , plotted in Figure 10.3-2. This function goes to zero on the axis, so electrons there do not interact with the circuit. Consequent-

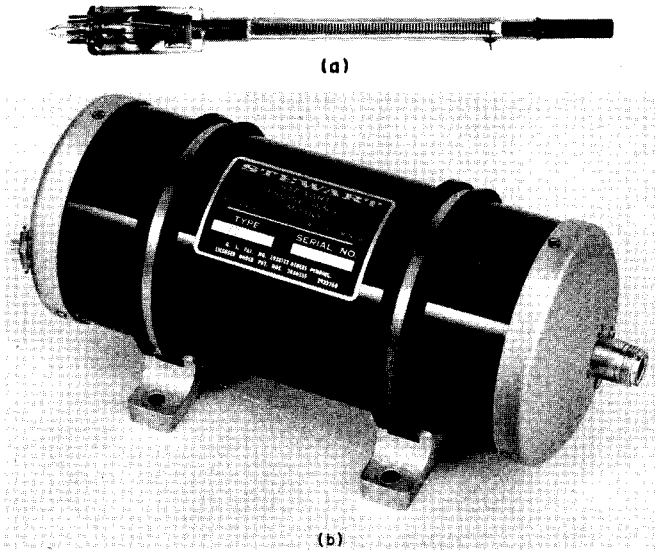


FIG. 11.2-4 SE 201 backward-wave oscillator. (a) Vacuum tube alone, without rf output coupling and focusing magnet. (b) Complete package of tube in permanent magnet. The package is 22 cm long and 11 cm in diameter. (Courtesy of Stewart Engineering Co.)

<sup>8</sup>Ibid.

ly, backward-wave oscillators are often built using hollow beams instead of solid ones.<sup>9</sup>

As an example of a practical backward-wave oscillator, let us consider the Stewart Engineering Company SE 201, shown in Figure 11.2-3. Photographs of the tube are shown in Figure 11.2-4. This tube delivers a minimum of 10 mw of power electronically tunable over the frequency range 7 to 12.4 Gc. The power output and helix voltage as a function of frequency are shown in Figure 11.2-5 for a beam current of 7 milliamps. The electron

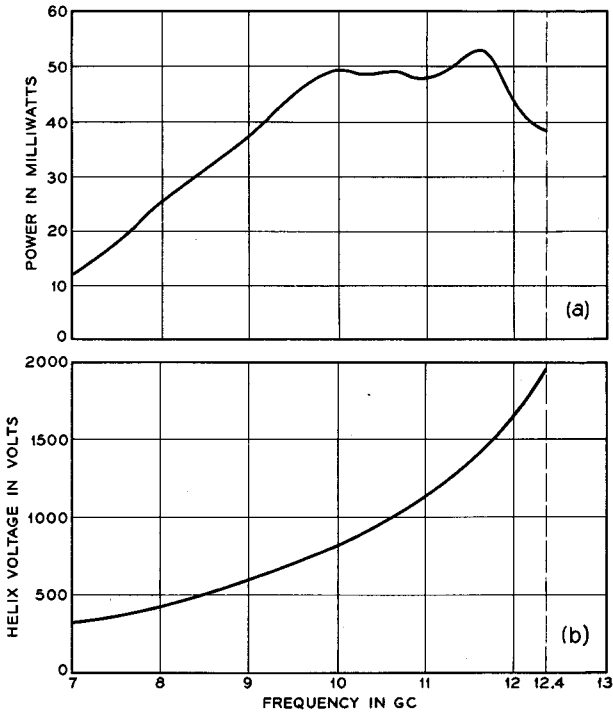


FIG. 11.2-5 Electrical characteristics of the SE 201 for a constant beam current of 7 ma. (a) Power output vs. frequency. (b) Tuning curve, helix voltage vs. frequency. (Courtesy of Stewart Engineering Co.)

beam is hollow, with an outer diameter of 2.9 mm and an inner diameter of 2.4 mm. The power may be varied by means of a control grid in the electron gun, which varies the beam current. Amplitude modulation is obtained in

<sup>9</sup>Space-charge reduction factors for hollow beams are given in Reference 9.3.

this manner. The collector is cooled by heat conduction to the envelope of the package.

The helix is a molybdenum tape, 0.127 mm thick and 0.508 mm wide. The tape is wound into a helix with an inside diameter of 3.2 mm and a pitch of 1.06 mm. At the highest operating frequency,  $ka = 0.416$ .

The tube is packaged in a permanent magnet; the complete package weighs 11 pounds. The electron beam is focused using confined flow as described in Section 3.4(b); that is, the magnetic field is relatively uniform from the cathode to the collector. The permalloy rings help to provide a uniform magnetic field as in the tube of Figure 10.3-7. The gun end of the helix is connected to the center conductor of a coaxial cable for rf output power by means of a pin through the glass envelope of the tube.

A lossy material is applied at the collector end of the helix so as to provide an internal rf termination. The pin connection at this end of the helix is for connection to the helix dc power supply.

An important characteristic of oscillators is the relative strength of the desired output signal as compared with all other spurious frequencies. The desired signal in this tube is at least 60 db larger than the total power in all spurious signals. Backward-wave oscillators in general produce extremely clean output signals.

The chief disadvantage of the backward-wave oscillator is its low electronic efficiency. At the highest frequency at which the SE 201 operates the tube has an electronic efficiency of only 0.3 per cent. On the other hand, the backward-wave oscillator provides a wider electronic tuning range than any other microwave tube. The backward-wave oscillator has been built at higher frequencies than any other microwave tube; power outputs of a few milliwatts have been obtained at 500 Gc.

### 11.3 Backward-Wave Amplifiers

The backward-wave oscillator may be used as a backward-wave amplifier, provided that rf coupling is furnished at the collector end of the helix for application of the input signal. The beam current is adjusted to a value below the current needed to start oscillation. The amplified output signal is taken from the gun end of the helix.

The helix voltage is adjusted as indicated in Figure 11-2. Amplification is obtained at the frequency of synchronism with the  $-1$  space harmonic. As the signal frequency is varied from the synchronous value, the space-harmonic phase velocity departs from the beam velocity much faster than in a forward-wave amplifier. As a result, backward-wave amplifiers have much narrower fractional bandwidths, typically 0.1 to 1 per cent.

The voltage gain of a backward-wave amplifier is given by the reciprocal

of the right-hand side of Equation (11.1-15). For a particular tube, at the beam voltage and frequency corresponding to synchronism, the right-hand side of Equation (11.1-15) is a function of the beam current,  $F(I_o)$ . At start oscillation it is equal to zero,

$$F(I_{ST}) = 0 \tag{11.3-1}$$

We can find an approximate expression for the gain as a function of beam current by expanding  $F(I_o)$  in a Taylor series about the starting current. That is,

$$F(I_o) \cong F(I_{ST}) + \left[ \frac{\partial F}{\partial I_o} \right]_{I_{ST}} (I_o - I_{ST}) \tag{11.3-2}$$

In taking the partial derivative, we make the simplifying assumption that the total change in  $F$  with current is due to the change in  $C$  in each exponent. Thus, we neglect the variations in the  $\delta$ 's and  $QC$ . Using this approximation, one obtains:

$$F(I_o) = \frac{I_o - I_{ST}}{I_{ST}} \frac{2\pi CN}{3I_{ST}} \left[ \frac{\delta_1(\delta_1^2 + 4QC)}{(\delta_1 - \delta_2)(\delta_1 - \delta_3)} e^{2\pi\delta_1 CN} + \frac{\delta_2(\delta_2^2 + 4QC)}{(\delta_2 - \delta_3)(\delta_2 - \delta_1)} e^{2\pi\delta_2 CN} + \frac{\delta_3(\delta_3^2 + 4QC)}{(\delta_3 - \delta_1)(\delta_3 - \delta_2)} e^{2\pi\delta_3 CN} \right] \tag{11.3-3}$$

where all the parameters are evaluated at  $I_{ST}$ . The gain may thus be written as

$$\text{gain} = 20 \log \frac{1}{|F(I_o)|} \text{db} = 20 \log \frac{k'}{1 - \frac{I_o}{I_{ST}}} \text{db} \tag{11.3-4}$$

where  $k'$  is a function of the helix loss and the space-charge parameter, as defined by the last two equations. Values of  $k'$  are given in Table 11.3-1 for zero helix loss and various values of  $QC$ . Maximum gain is obtained for  $QC$  in the neighborhood of 0.5. Equation (11.3-4) is plotted in Figure 11.3-1 for  $QC = 0$ .

TABLE 11.3-1

$QC$	$k'$
0	1.01
0.25	1.22
0.50	2.03
0.75	1.71
1.00	1.83
1.50	1.68

Examination of Figure 11.3-1 reveals that appreciable gain is achieved only for beam currents extremely close to the starting current value. In addition, slight variations in the beam current produce large fluctuations in

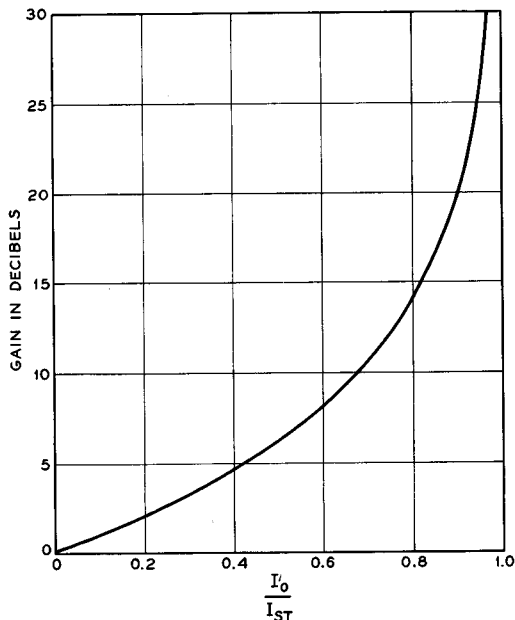


Fig. 11.3-1 Theoretical gain of a single helix backward-wave amplifier for  $QC = 0$ . The value of gain is the maximum value at the center of the amplification band. Appreciable amounts of gain are obtained only for beam currents just below the starting current,  $I_{ST}$ .

the gain at high-gain levels. This characteristic makes gain stability a serious problem. This is a consequence of operating so close to the point of oscillation. Since  $I_{ST}$  generally increases with frequency, the gain at constant beam current generally decreases with frequency.

Another disadvantage of this device is the lack of discrimination against signals outside the amplifying passband. All signals may propagate along the helix from the input to the output without any attenuation other than the normal helix attenuation. This latter attenuation is kept as small as possible so as to obtain maximum gain at the operating frequency. In contrast, the circuit sever in the forward-wave amplifier provides 60 db or more of attenuation to signals outside the amplifying band.

These disadvantages are eliminated in the device shown in Figure 11.3-2,

the cascade backward-wave amplifier.<sup>10</sup> This device is evolved from the single-helix backward-wave amplifier by using two helices of equal length. Each helix has one end terminated as shown. This procedure is analogous to the transition from a two-cavity to a three-cavity klystron amplifier.

The amplifier functions in the following manner. The first helix acts as a single-helix backward-wave amplifier, with the amplified circuit power being dissipated in a termination at the gun end of the helix. The modulation

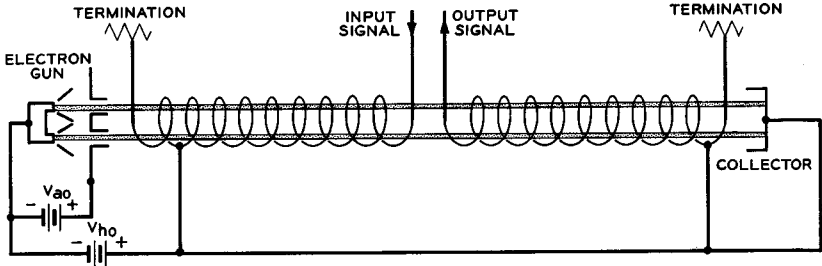


FIG. 11.3-2 The cascade backward-wave amplifier.

produced on the beam by the first helix is carried by space-charge waves to the second helix, where backward-wave interaction produces additional gain. The output signal is removed from this helix as shown in Figure 11.3-2. Because of the physical separation between the two helices, the input and output ports of the tube are effectively isolated for frequencies outside of the amplification band.

It may at first appear that the gain of the cascade amplifier is merely twice the gain in db obtained on the first helix. However, this is not the case; the gain of the second helix is considerably larger than that of the first helix. This is due to the fact that the beam is premodulated upon entering the second helix, resulting in enhanced interaction and larger overall gain. As an example, for a beam current of one-half the starting current for either helix, the gain in the first helix is 6 db, whereas the gain in the second helix is 15 db. These theoretical values are for  $QC = d = 0$ . In this case, an overall gain of 21 db is obtained for a beam current considerably below the starting current.

Experimental curves for the gain of a particular cascade backward-wave amplifier are shown in Figure 11.3-3.<sup>11</sup> The variation of gain with beam current is much less severe than in the case of a single-helix tube, for equal overall gains. One drawback of the backward-wave amplifier is evident

<sup>10</sup>Reference 11.5.

<sup>11</sup>*Ibid.*

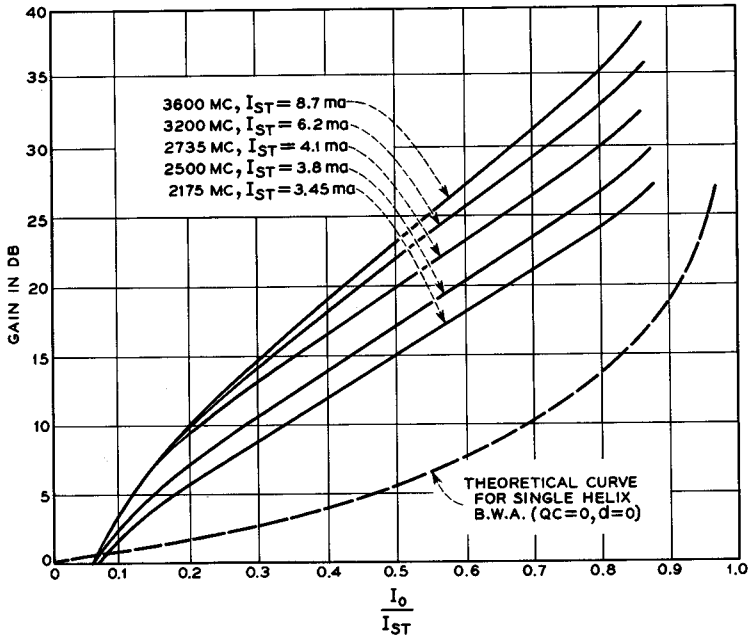


FIG. 11.3-3 Experimental measurements of gain in a cascade backward-wave amplifier. Appreciable values of gain are obtained for beam currents considerably below the starting current. The helix voltage is adjusted for maximum gain at each frequency (Reference 11.5). (Courtesy of *Proceedings IRE*)

from these curves. The maximum gain varies considerably with frequency for a constant beam current. For a beam current of 3 ma, the gain varies from 17 to 27 db for the frequencies indicated in the figure.<sup>12</sup> Constancy of maximum gain can be achieved by varying the beam current in conjunction with the helix voltage.

The cascade backward-wave amplifier is thus seen to overcome the most serious drawbacks of the single helix version. As a result, we have a practical device for those applications requiring a narrow-band amplifier, voltage tunable over a wide frequency range.

### PROBLEMS

11.1 An idealized, lossless slow-wave structure has a Brillouin diagram whose fundamental or zero-order space harmonic is a straight line between the points

<sup>12</sup>Thus at 2175 Mc the starting current is 3.45 ma. For a beam current of 3.0 ma,  $I_o/I_{ST} = 3.0/3.45 = 0.87$ , and the corresponding gain is 27 db. On the other hand, at 3600 Mc a beam current of 3.0 ma gives  $I_o/I_{ST} = 3.0/8.7 = 0.34$ . The corresponding gain is 17 db.

$\beta L = 0$ ,  $\omega = \omega_o/2$  and  $\beta L = \pi$ ,  $\omega = \omega_o$ . The axial component of the electric field is given by the expression

$$E_z(x,y,z) = \frac{\sqrt{P} \left( \frac{\mu_o}{\epsilon_o} \right)^{1/4}}{10L} \sum_{-\infty}^{\infty} \frac{\epsilon^{-i\beta_n z}}{n^2 + 1}$$

where

$$\beta_n = \beta_o + \frac{2\pi n}{L}$$

and  $P$  is the total power flow for a propagating mode.

- (a) Sketch the Brillouin diagram over the range  $-2\pi \leq \beta L \leq 2\pi$ . Indicate typical points of operation for traveling-wave amplifiers and backward-wave oscillators.
- (b) Derive expressions for the beam-coupling impedances for fundamental and backward-wave interaction.
- (c) In operation as a forward-wave amplifier the beam voltage is pulsed up to give synchronous interaction with the fundamental space harmonic. During the rise time of this voltage pulse, the electron velocity is synchronous with the phase velocity of the backward wave, and there is the possibility of backward-wave oscillations. Derive an expression for  $CN$  for the backward wave as a function of the variables  $\omega$  and  $\beta_o$ , assuming  $\beta_{-1} = \beta_o$  (small  $C$ ). The ratio of  $I_o$  to  $V_o^{3/2}$  remains constant during the rise time of the voltage.
- (d) What is the maximum gain of the traveling-wave amplifier at the frequency  $\omega = \frac{3}{2}\omega_o$ , limited by the criterion that backward-wave oscillations are not produced during the rise time of the beam voltage pulse? Assume small  $C$ , and  $QC = d = 0$ .  $b = 0$  for the amplifier. The circuit is perfectly matched at both ends. Ans.: 11.9 db.

11.2 Show that  $M_{2(-1)}^2$  in Equation (11.2-9) for an annular beam in a helix is given by

$$M_{2(-1)}^2 = \frac{b^2[I_1^2(\gamma_{-1}b) - I_o(\gamma_{-1}b)I_2(\gamma_{-1}b)] - c^2[I_1^2(\gamma_{-1}c) - I_o(\gamma_{-1}c)I_2(\gamma_{-1}c)]}{(b^2 - c^2)I_1^2(\gamma_{-1}a)}$$

where  $a$  is the helix radius,  $b$  is the outer beam radius, and  $c$  is the inner beam radius. The following expressions will be helpful:

$$I_{-1}(ax) = -I_1(ax)$$

$$\int r I_1^2(ax) dr = \frac{r^2}{2} [I_1^2(ax) - I_o(ax)I_2(ax)]$$

11.3 A tape helix backward-wave oscillator is to be designed to oscillate at 9 Ge. Find the helix length and beam current necessary for oscillations to start at a beam voltage of 2500 volts, using Figures 11.1-3 and 11.1-4, assuming negligible helix loss. Assume the electron beam is a thin annular beam just grazing the helix, so that  $M_{2(-1)} = 1$ ; assume  $\delta/L = \frac{1}{3}$  so that the helix impedance is given by Equation



(11.2-9) as plotted in Figure 11.2-2. The following parameters are also given:

$$\begin{aligned} \text{Helix radius } a &= 2.54 \text{ mm} \\ \cot \psi &= 10 \\ \text{Space-charge reduction factor } R &= 0.4 \\ \text{Beam cross-sectional area} &= 4 \text{ mm}^2 \\ \text{Ans.: } &2.06 \text{ cm, } 49.6 \text{ ma.} \end{aligned}$$

11.4 Calculate the power output for the backward-wave oscillator of the previous problem at beam currents of 60 ma, 100ma, and 200 ma.

11.5 For large values of the space-charge parameter  $QC$ , the incremental propagation constants of a backward-wave oscillator are given by Equations (11.1-21).

- (a) Show that the magnitudes of the convection current and the  $z$  component of the electric field due to the circuit at the threshold of oscillation are given as functions of  $z$  by the equations:

$$\begin{aligned} |i(z)| &= |i(l)| \sin \frac{1}{2}\beta_e C(QC)^{-1/4}z \\ |E_{zn}(z)| &= |E_{zn}(0)| \cos \frac{1}{2}\beta_e C(QC)^{-1/4}z \end{aligned}$$

- (b) From the results of part (a) show that the starting value of  $CN$  is given by

$$CN = \frac{1}{2}(QC)^{1/4}$$

- (c) If the beam current is made much larger than the value necessary to start oscillations, the backward-wave oscillator will oscillate in a higher-order mode. Assuming that this higher order mode occurs at the same frequency and beam voltage as the fundamental mode of oscillation, show from the results of part (a) that it occurs at a beam current equal to 81 times the starting value for the fundamental mode of oscillation.

### REFERENCES

Three general references on backward-wave interaction are:

- 11a. H. Heffner, "Analysis of the Backward-Wave Traveling-Wave Tube," *Proc. IRE* **42**, 930-937, June, 1954.
- 11b. A. H. W. Beck, *Space-Charge Waves and Slow Electromagnetic Waves*, Pergamon Press, Inc., New York, pp. 241-255, 1958.
- 11c. R. Kompfner and N. T. Williams, "Backward-Wave Tubes," *Proc. IRE* **41**, 1602-1611, November, 1953.

References covering specific items discussed in the chapter are:

- 11.1 H. R. Johnson, "Backward-Wave Oscillators," *Proc. IRE* **43**, 684-697, June, 1955.
- 11.2 R. W. Grow, and D. A. Watkins, "Backward-Wave Oscillator Efficiency," *Proc. IRE* **43**, 848-856, July, 1955.
- 11.3 D. A. Watkins, and E. A. Ash, "The Helix as a Backward-Wave Circuit Structure," *J. Appl. Phys.* **25**, 782-790, June, 1954.
- 11.4 P. K. Tien, "Bifilar Helix for Backward-Wave Oscillators," *Proc. IRE* **42**, pp. 1137-1143, July, 1954.
- 11.5 M. R. Currie and J. R. Whinnery, "The Cascade Backward-Wave Amplifier: A High-Gain Voltage-Tuned Filter for Microwaves," *Proc. IRE* **43**, 1617-1631, November, 1955.